photonics

MDPI

Article

Realization of 4 × 200 Gbps 4-QAM OFDM-OWC System Using Higher Order OAM Modes for HAP-to-Satellites Scenario

Meet Kumari [1] and Satyendra K. Mishra [2,*]

[1] Department of Electronics & Communication Engineering, University Institute of Engineering, Chandigarh University, Gharuan, Mohali 140413, India; meetkumari08@yahoo.in
[2] SRCOM, Centre Technologic de Telecomunicacions de Catalunya, 08860 Castelldefels, Barcelona, Spain
* Correspondence: smishra@cttc.es

Abstract: Recently, there has been an increase in interest in using optical wireless communication (OWC) links on high-altitude platforms (HAPs) for satellite applications. We implement an orbital angular momentum (OAM) multiplexed orthogonal frequency division multiplexing (OFDM) system using an OWC link. A space-to-air scenario is considered in which transmission pointing errors, geometric loss, turbulence, and additional link losses are taken into account to extend the transmission range, system capacity, and throughput. At 200 Gbps per channel data rate, four different OAM modes are implemented with higher order Laguerre–Gaussian (LG) modes of [0,0], [0,13], [0,40], and [0,80]. An aggregate 800 Gbps data rate can deliver a maximum OWC range of 3300–5000 km for all channels. The maximum received power over the 1000 km range is −19.34 to −32.59 dBm with an additional gain of 0–2.5 dB. It is also possible to obtain a better performance over large distances of 500–3500 km with an error vector magnitude of 2.98–17.5%. Furthermore, a high gain of −40.80 dB, a signal-to-noise ratio (SNR) of 55.21 dB, and an optical SNR of 67.25 dB can be achieved for varied transmitter pointing errors of 0.1 rad. As compared to other literature, this system exhibits a superior performance.

Keywords: HAP; OAM; OFDM; satellite; LG modes

Citation: Kumari, M.; Mishra, S.K. Realization of 4 × 200 Gbps 4-QAM OFDM-OWC System Using Higher Order OAM Modes for HAP-to-Satellites Scenario. *Photonics* **2024**, *11*, 294. https://doi.org/10.3390/photonics11040294

Received: 28 February 2024
Revised: 19 March 2024
Accepted: 23 March 2024
Published: 25 March 2024

1. Introduction

Satellite communications technology has emerged as a key technology for offering fixed and mobile wireless services in disaster and remote areas due to its inherent advantages of wide service exposure and environmental immunity. The use of high aerial platforms (HAPs) as flying network nodes in aerial communications has attracted considerable attention from industry and academia at the same time, mainly because of their wide coverage and ease of deployment, particularly in disaster areas, marine communications, and provisional extensive events [1]. It is demanding to enhance the throughput and the coverage zone of a HAP-to-satellite communication, which is sensitive to weather-related problems. Additionally, the HAP-aided satellite will increase the scalability of the fifth-generation network and beyond. In a cloud-free environment, HAP is a quasi-fixed vehicle located at an altitude of 17–25 km above the Earth's surface [2].

Compared to radio frequency, optical wireless communications (OWCs) offer a license-free spectrum, reliable channel security, and high bandwidth, making them a promising scheme for future space communications [3]. The use of OWC link-based systems for HAP-aided satellites is critical to achieving highly efficient satellite scenarios. Due to the performance of these systems, turbulence-related scintillation caused by beam propagation through the atmosphere can be substantially minimized. In recent years, several techniques have been proposed to reduce scintillation's detrimental effects. Some techniques use relay schemes, which consider some factors that affect the communication link, such as non-coherent and coherent modulation schemes in orthogonal frequency division multiplexing (OFDM) [4].

The OFDM technique is an intriguing candidate for future optical wireless technologies with high bandwidth. This multicarrier communication technology transmits high-speed data by splitting them into parallel orthogonal channels at low speeds. OFDM offers the greatest spectral efficiency and facilitates dynamic bandwidth allocation for a variety of applications both in the frequency and time domains [5], providing a high-performance, flexible, reliable, transparent, and dynamically reconfigurable HAP-assisted system to meet these severe requirements. Over the past ten years, conventional optical satellite links have been developed and operated independently [6].

Due to its ability to mitigate the capacity crunch of existing deployed OWC links, mode division multiplexing (MDM) has gained a lot of traction as defined in [7–10], but also possesses design complexity as well as throughput. However, the benefit of MDM is that it allows more transmission links to be accessible within an OWC link. Thus, one of the most anticipated approaches that has currently gained special attention in OWC links for space communications is orbital angular momentum (OAM), which is also termed twisted light. The concept of OAM refers to the limitlessness and orthogonality of various modes of operation. OAM modes have proven strong in terabit-to-petabit scale potential transmission, and they have gained from a dozen to hundreds of percent spectral efficiency over OWC links [11]. Despite the numerous benefits of OAM in OWC links, there are several predominant issues which were not discussed earlier using higher-order OAM modes in previous works for HAP scenarios in [12–15]. These major issues need to be addressed such as (1) OAM beams mode crosstalk owing to smaller differences among various modes, (2) receiver low power efficiency caused by very high order Laguerre–Gaussian (LG) modes in OAM, (3) mode leakage as a result of pointing errors, and (4) significant phase modulation when turbulence is present. In OWC satellite links with HAP-assisted transmission, OAM beams have yet to be demonstrated over long distances at terabit throughput [16].

2. Literature Review

A study in [12] developed analytical expressions for analyzing the HAP relay footprint area, spectral efficiency, and capacity per user. Three distinct eavesdropping scenarios are presented and investigated for the security of physical layer performance in HAP systems. According to results, the eavesdropper signal-to-noise ratio (SNR), scattering proportion, distance, and zenith angle can be crucial factors in supporting communication security in HAP systems [13]. An integrated free space optics (FSO) and radio frequency (RF) downlink link is presented for data delivery via FSO link to relays. A reasonable tradeoff between service fairness and system capacity can be achieved according to the results [1]. The effects of atmospheric turbulence on Hoyt distribution misalignment fading have also been realized in another work [14]. The HAP scenario is investigated using an integrated space–air–ground network using FSO/RF links. In uplink transmission, integrated FSO/RF systems achieve optimum performance compared to FSO systems using backup RF links [15]. Moreover, the OAM scheme is experimentally validated in terms of antenna design at 5.5 GHz. Two new receiver SNR improvement approaches help eliminate mode-dependent performance degradation in the system [7]. We present a successful OAM-based satellite communication system using three OAM beams over a 22,000 km OWC link in [16]. In addition, a wavelength division multiplexing (WDM) system using OAM multiplexing is presented. It is possible to achieve a BER of 10^{-9} with 1.4 dB power penalty by using OAM beams at 1.6 Tbps [8]. There is a proposal for an 1120-channel MDM-OAM-WDM system over a 100 km ring-core fiber [9]. The performance of 64-quadrature amplitude modulation (QAM) OFDM over multicasting links is demonstrated. The results indicate a favorable performance in terms of BER and optical signal-to-noise ratio (OSNR) [10].

According to these works, researchers mostly focused on individual HAP scenarios using OWC links, OFDM-OAM based systems, or hybrid FSO/RF systems. OAM-HAP assistance in satellite systems was only considered in a small number of these studies. Fur-

thermore, the presented systems do not use the most advantageous modulation technique for multiple users, which is OFDM over satellite-to-HAP. Moreover, little has been done to enhance distance and throughput in such systems for future satellite communication networks. Therefore, OAM-OFDM using OWC links is proposed and investigated for next-generation high-capacity space-to-satellite communication to address network operators' demands. This work makes the following major contributions: To design high-speed and high-capacity OAM modes operated 4-QAM OFDM using OWC link for HAP-to-satellite scansions.

- To investigate the system performance over long-reach transmission at 200 Gbps for four operating modes viz. LG [0,0], LG [0,13], LG [0,40] and LG [0,80].
- To evaluate the system performance in terms of error vector magnitude (EVM), signal power, SNR, and OSNR.
- To validate the system performance with existing ones.

This paper is organized as follows: Section 3 describes the system design demonstrating the system block diagram and generated OAM modes. Then, Section 4 depicts the performance evaluation of the proposed work with mathematical analysis. The conclusion and future scope are presented in Section 5.

3. Proposed Design

The systematic block diagram of the proposed design of the 4-QAM ODFM-OWC system using different OAM modes is shown in Figure 1. The generated four different OAM modes used in the system are presented in Figure 2. The system is designed in OptiSystem v.21.

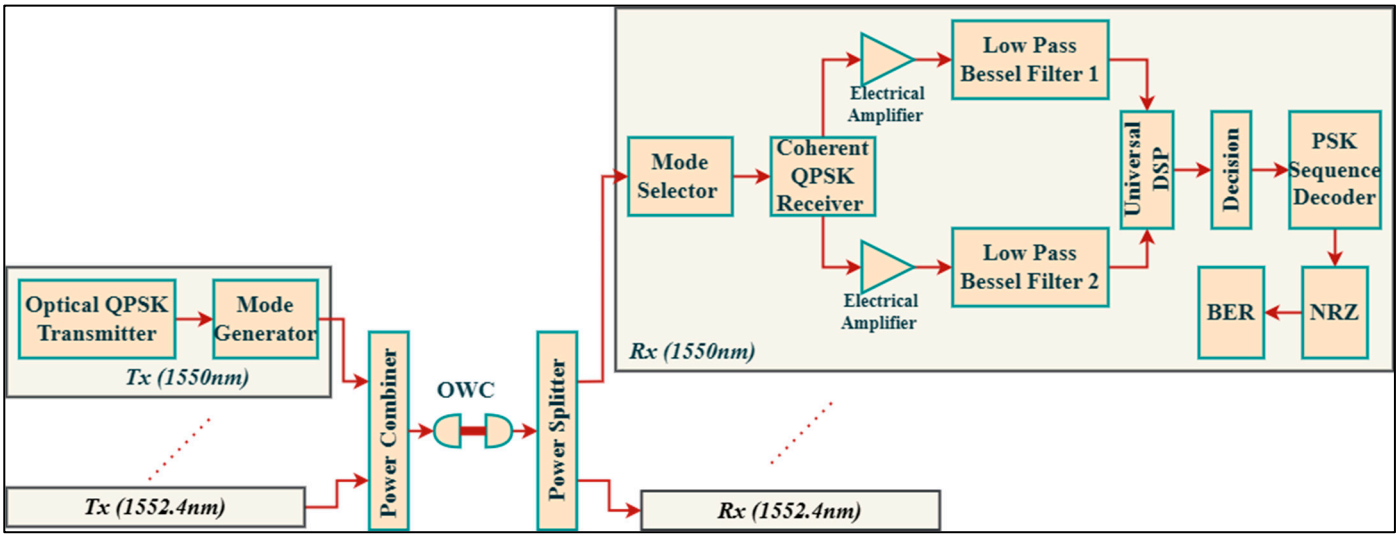

Figure 1. Systematic diagram of 4-QAM ODFM-OWC system using different OAM modes.

This design uses four transmitters operating at wavelengths of 1550, 1550.8, 1551.6, and 1552.4 nm. There are four higher-order OAM modes: LG [0,0], LG [0,13], LG [0,40], and LG [0,80] are realized at 1550 nm, 1550.8 nm, 1551.6 nm, and 1552.4 nm, respectively. Figure 1 illustrates an optical quadrature phase shift keying (QPSK) transmitter consisting of a laser at a specific wavelength modulated by a 4-QAM OFDM signal. Laser phase noise is modeled incorporating the probability density function as follows [17].

$$g(\Delta\epsilon) = \frac{1}{2\pi\sqrt{\Delta f dt}}\, e^{-\frac{\Delta\epsilon^2}{4\pi\Delta f dt}} \tag{1}$$

where $\Delta\epsilon$ means two subsequent time instants phase difference and dt means the time discretization. A non-return-to-zero QPSK signal at 100 Gbps data traffic is generated by a

pseudo random binary sequence generator of length 2^7–1 and a Mach–Zehnder modulator. The laser has a linewidth of 0.1 MHz and is set at a definite wavelength with an output power of 20 dBm. An LG mode generator is incorporated to generate a specific LG mode and the generated QPSK mode signal is sent to the MDM-OWC link.

An OWC link transmits the combined power from all incoming transmitters modulating different OAM signals using a power combiner. The OWC link is considered a link between the HAP and the satellite, which is located 20 km above the surface. Power splitters divide incoming optical signals into different receivers for mode sectioning and demodulation. After propagation over the OWC link, the four modes are separated via a mode selector and then sent to a data-recovery setup. A coherent optical QPSK receiver uses a PIN photodetector to convert light signals into electrical signals. It incorporates a bandwidth of 22 GHz, output power of 10 dBm, responsivity of 1 A/W and an 8 nA dark current. Through a pair of electrical amplifiers having a gain of 20 dB, the received electrical signal is amplified and passed through a pair of low-pass Bessel filters [17].

To support the recovery of incoming signals after coherent detection, a single polarization universal digital signal processing module is incorporated. A decision component is used to evaluate the performance of the system in terms of EVM% and symbol error rate. Phase shift keying (PSK) sequence generators represent antipodal signals in binary phases 00 (binary '0′) and 1800 (binary '1′). In addition, a BER analyzer is used to evaluate the system performance using the NRZ modulation format [17].

LG modes are circularly symmetric as well as directly concerned with the quantized OAM of electrons and photons. For these reasons, the LG modes plays a significant role in several areas of physics. Also, LG modes are utilized for quantum optics, quantum memories, telecommunications, and much else [18]. LG modes effectively strengthen the OWC range and offer more flexibility to a turbulence-induced atmosphere as compared to Hermite–Gaussian (HG) modes. Furthermore, in comparison with HG modes, LG modes pose a higher channel capacity and more robustness despite the beam without effecting the detection. LG beams are exclusive information-carriers, which are selected to improve the larger freedom for transmitting signals. These beams also support data encoding in amplitude and phase, which offer more system reliability under severe atmospheric conditions. Again, four LG modes over the OWC link under atmospheric turbulence are represented as [17]:

$$\delta_{r,l}(\theta, \varnothing) = \beta \left(\frac{2\theta^2}{\mu_0^2} \right)^{\frac{\rho}{2}} . L_r^l \left(\frac{2\rho^2}{\mu_0^2} \right) . exp \left(\frac{-\rho^2}{\mu_0^2} \right) . exp \left(\frac{\pi \rho^2}{\lambda S_0} \right) \begin{cases} \cos(l\varnothing), & l < 0 \\ \sin(l\varnothing), & l \geq 0 \end{cases} \quad (2)$$

where θ is the curvature radius, r and l mean modes dependencies along the x-and y-axis, respectively, μ is the spot size, L_r and L_l stand for Laguerre polynomials, S_0 is the normalized radius, λ is the operating wavelength, ρ and β are the beam divergence as well as the considerable atmospheric attenuation coefficient. Table 1 describes various components' parameters and values.

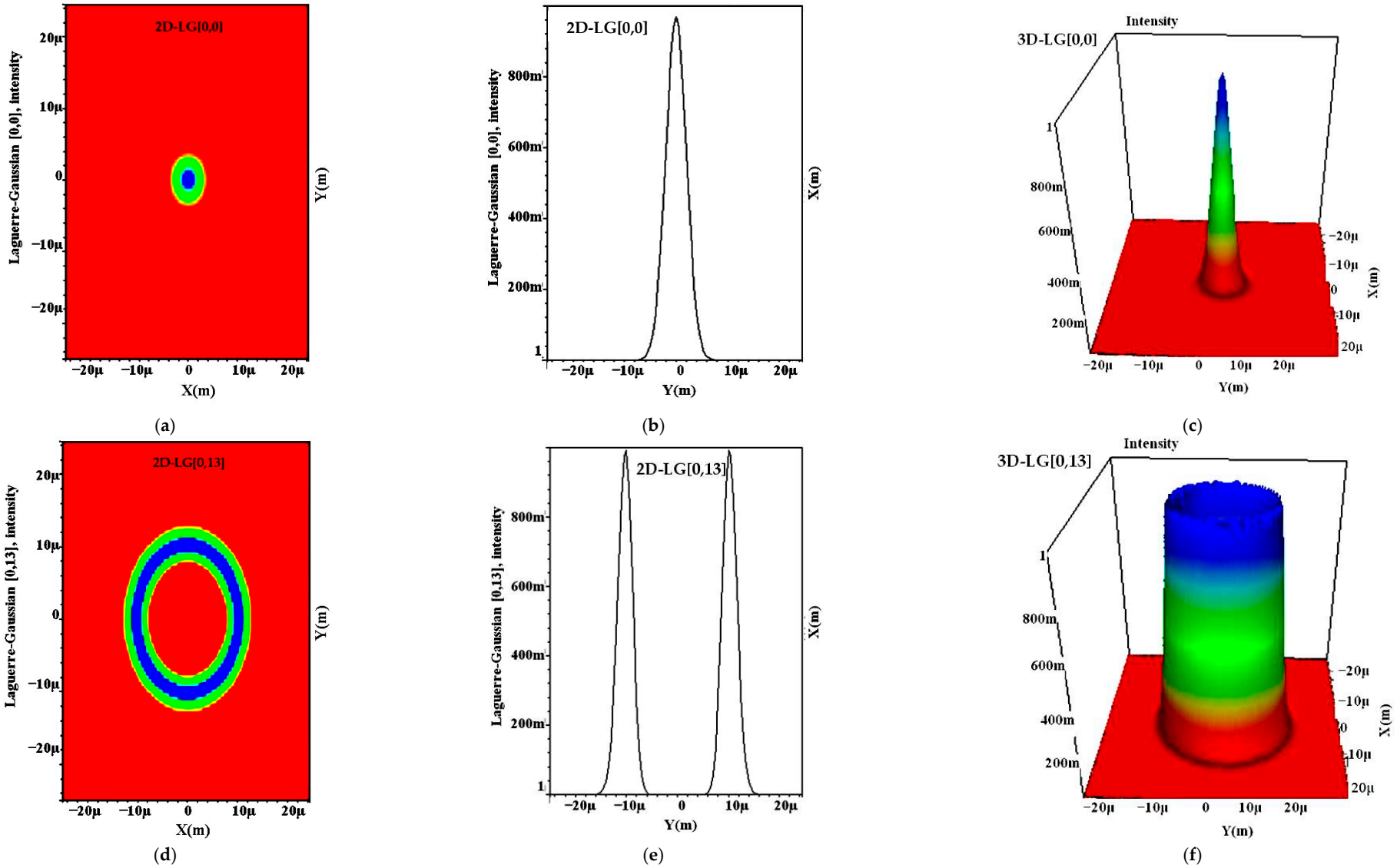

Figure 2. *Cont.*

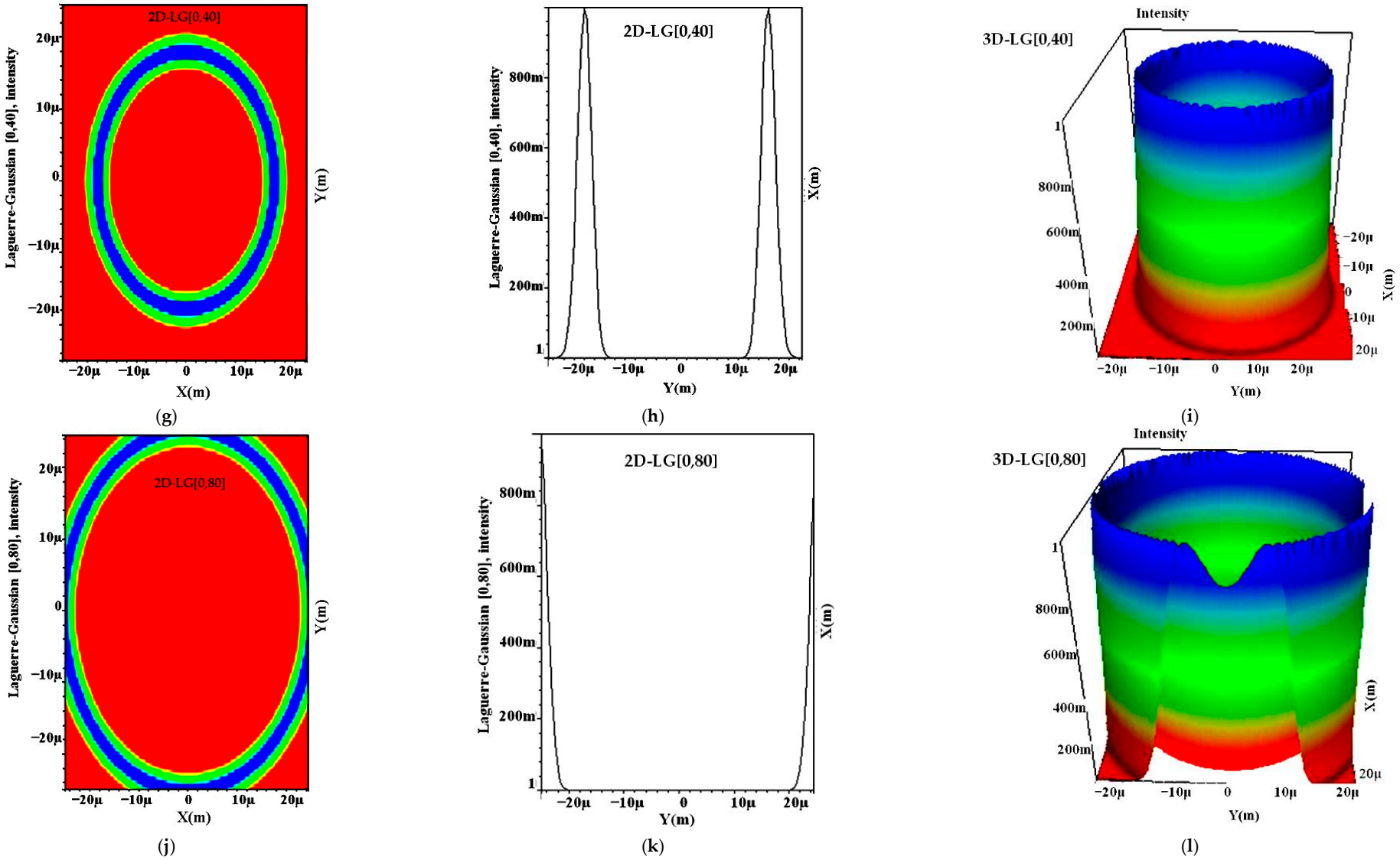

Figure 2. Generated LG modes profile's view in 2D and 3D.

Table 1. Components' parameters values [17,19].

Component	Parameters	Value	Unit
QPSK transmitter	Wavelength	1550, 1550.8, 1551.6, 1552.4	nm
	Data rate	200	Gbps
	Power	20	dB
	Linewidth	0.1	MHz
	Azimuth	45	deg
OWC channel	Reference wavelength	1550	nm
	Range	500–5000	km
	Tx and Rx aperture diameter	15	cm
	Tx and Rx optics efficiency	0.8	
	Free space path loss	Yes	
	Geometric gain	Yes	
	Tx and Rx pointing error	0–1	μrad
	Additional losses	0–2.5	dB
QPSK Receiver	Wavelength	1550, 1550.8, 1551.6, 1552.4	nm
	Power	10	dB
	Responsivity	1	A/W
	Dark current	8	nA
Electrical amplifier	Gain	20	dB
Low pass Bessel filter	Cut-off frequency	0.75 × Bit rate	Hz
PSK sequence decoder	Bits per symbol	2	

4. Results and Analysis

To evaluate the system's performance, BER, eye diagrams, constellation diagrams, received power, optical and electrical spectra, and OAM modes were considered. Mathematically, BER performance in terms of EVM is defined as [17]:

$$BER_{m-QAM} = erfc\left(\sqrt{\frac{1}{EVM^2} \times \frac{3}{2(m-1)}}\right) \cdot \frac{2}{log_2(m)}\left(1 - \frac{1}{\sqrt{m}}\right) \quad (3)$$

where m is the modulation level i.e., four in this work. In addition, the SNR and $OSNR$ can be presented as [17]:

$$SNR(dB) = 10.log_{10}\left[\frac{P_s(mW)}{P_n(mW)}\right] \quad (4)$$

where P_s and P_n depict the signal and noise power, respectively.

$$OSNR(dB) = 10.log_{10}\left[\frac{P_s(mW)}{P_{n0.1}(mW)}\right] \quad (5)$$

where $P_{n0.1}$ means noise power within a 0.1.

A series of BER plots are shown in Figure 3a–d for different modes and distinct wavelengths as a function of the OWC range. Based on Figure 3a, LG [0,0] mode offers the best BER performance followed by LG [0,13], LG [0,40], and LG [0,80]. In the fundamental LG [0,0] mode, the maximum optical energy is transmitted. To present the optimal transmission range of the system, the BER limit of 10×10^{-3} is marked as a threshold limit. The best performance of the system is achieved at 1550 and 1550.8 nm wavelengths for all modes due to less impact of link impairments for these wavelengths. This is followed by an optimum performance at 1551.6 nm and then a worst performance at 1552.4 nm in terms of long-reach signals transmission. However, the system's performance can be enhanced by increasing the channel spacing and launch power and decreasing the data traffic. Notably, as shown in Figure 3a, the system provides the best BER when the range

is 500–5000 km for LG [0,0] for all operating wavelengths. LG [0,13] mode can achieve a maximum transmission range of 3700–5000 km at the BER limit as depicted in Figure 3b. In Figure 3c,d, it is shown that for higher modes, i.e., LG [0,40] and LG [0,80], the maximum range is 3500–5000 km and 3300–5000 km, respectively. Moreover, OAM modes generated are presented in Figure 3a–d over a 5000 km range, at the BER limit.

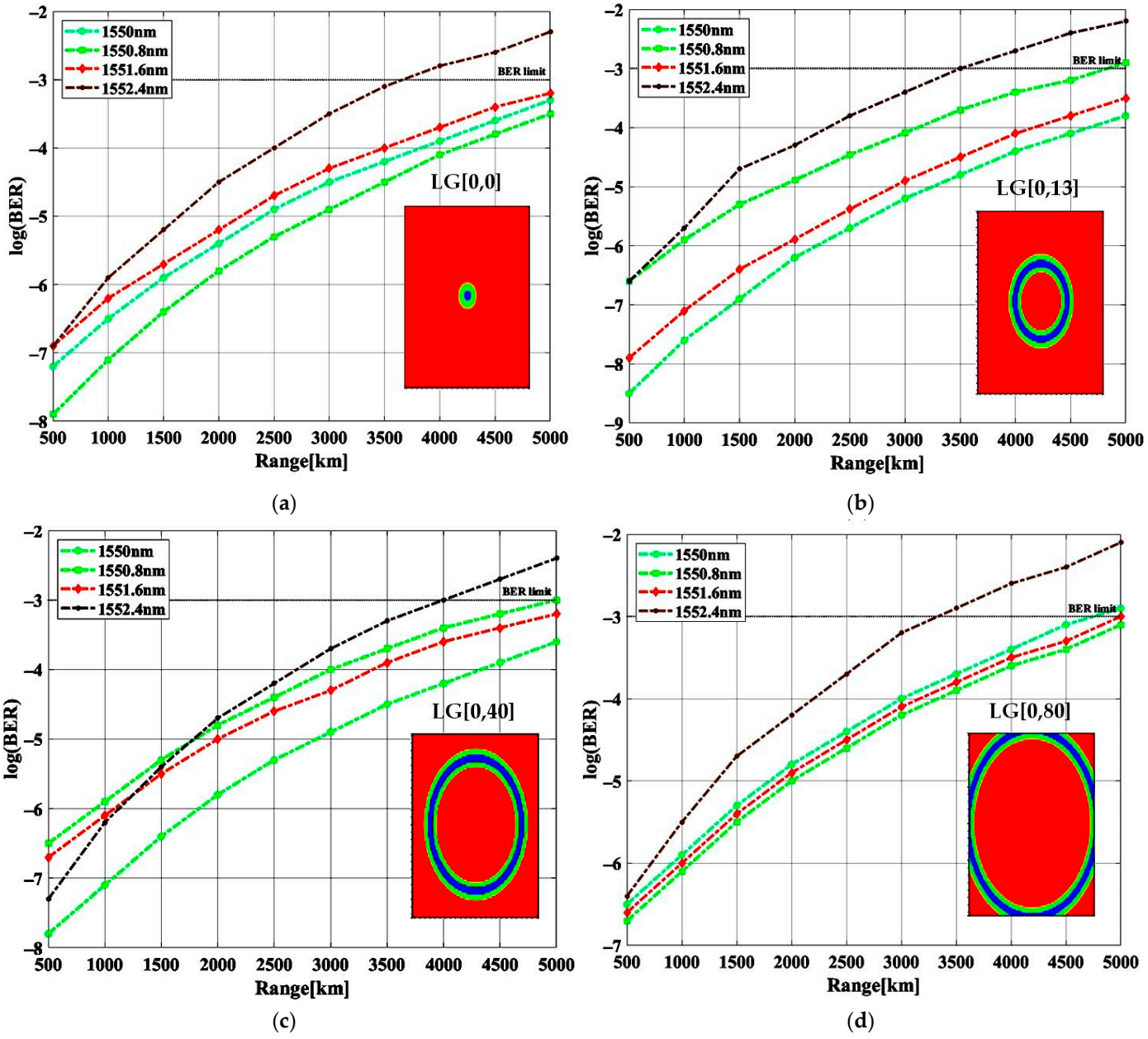

Figure 3. BER versus OWC range for operating modes of (**a**) LG [0,0], (**b**) LG [0,13], (**c**) LG [0,40] and (**d**) LG [0,80]; Insets: corresponding OAM modes.

Figure 4a–f illustrates the constellation diagrams for back-to-back and various modes at modes over a 5000 km range. As can be seen, clear and distortion-free constellations are obtained for LG [0,0] mode over a 1000–5000 km range when compared with back-to-back. However, other modes indicate signal distortions and thus low signal quality. These diagrams confirm that the proposed system can reduce atmospheric losses and turbulence in space communication. The maximum range achieved for different modes and wavelengths is shown in Table 2.

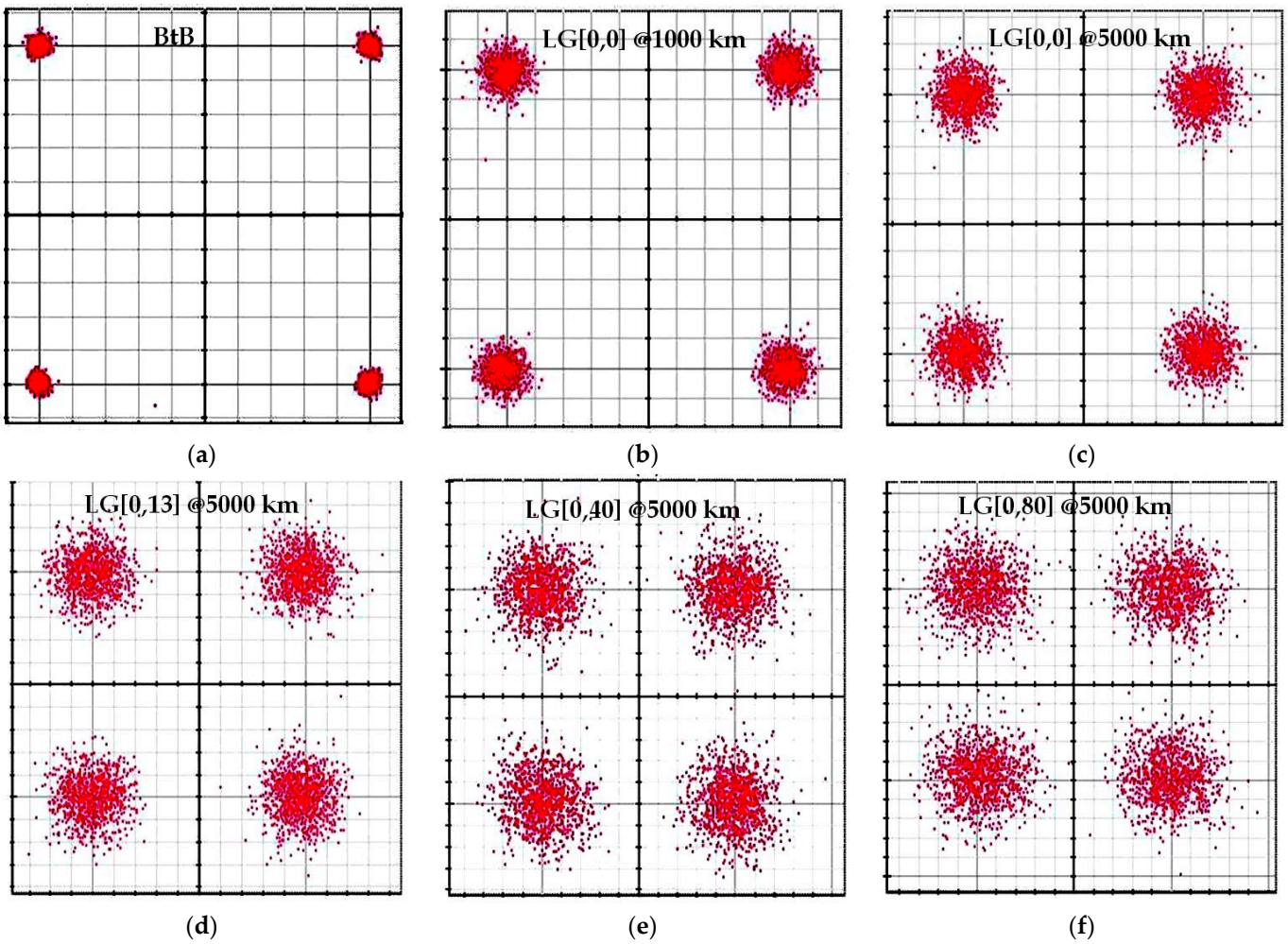

Figure 4. Constellation diagrams for (**a**) BtB, (**b**) LG [0,0] at 1000 km, (**c**) LG [0,0] at 5000 km, (**d**) LG [0,13] at 5000 km, (**e**) LG [0,40] at 5000 km and (**f**) LG [0,80] at 5000 km.

Table 2. Maximum obtained range for different modes and wavelengths @ BER limit.

Wavelengths (nm)	LG [0,0]	LG [0,13]	LG [0,40]	LG [0,80]
1550	5000	5000	5000	4000
1550.8	5000	5000	5000	3700
1551.6	5000	5000	4800	3500
1552.4	5000	5000	4700	3300

Figure 5a–d shows the received power versus additional losses for different LG modes over a range of 1000–4000 km. As the transmission range increases, all modes perform equally, which means that the optical power received decreases. Turbulence and link losses are responsible for this. Furthermore, the performance drastically changes for high additional losses in OWC links. In this case, fundamental mode LG [0,0] can approach superior performance over the entire range of additional losses. Because the fundamental mode transmits signal energy at the highest rate (99%) it is preferred. Consequently, a minimum received power of −19.34, −25.37, −28.89, and −31.39 dBm is obtained for 1000, 2000, 3000, and 4000 km ranges at 2.5 dB additional loss for LG [0,0] mode, as illustrated in Figure 5a. According to Figure 5b, the OWC range of 1000, 2000, 3000, and 4000 km offers received power of −19.45, −25.57, −29.19, and −31.79 dBm at 2.5 dB loss, respectively. For higher modes, the received power diminishes again. LG [0,40] and LG [0,80] offer received power of −19.54 and −19.64 dBm over 1000 km, −25.77 and −25.97 dBm over 2000 km,

−20.49 and −29.79 dBm over 3000 km and −32.19 and −32.59 dBm over 4000 km, at 2.5 dB loss, as presented in Figure 5c,d. The results demonstrate that even in the presence of link losses, a reliable communication range can be achieved.

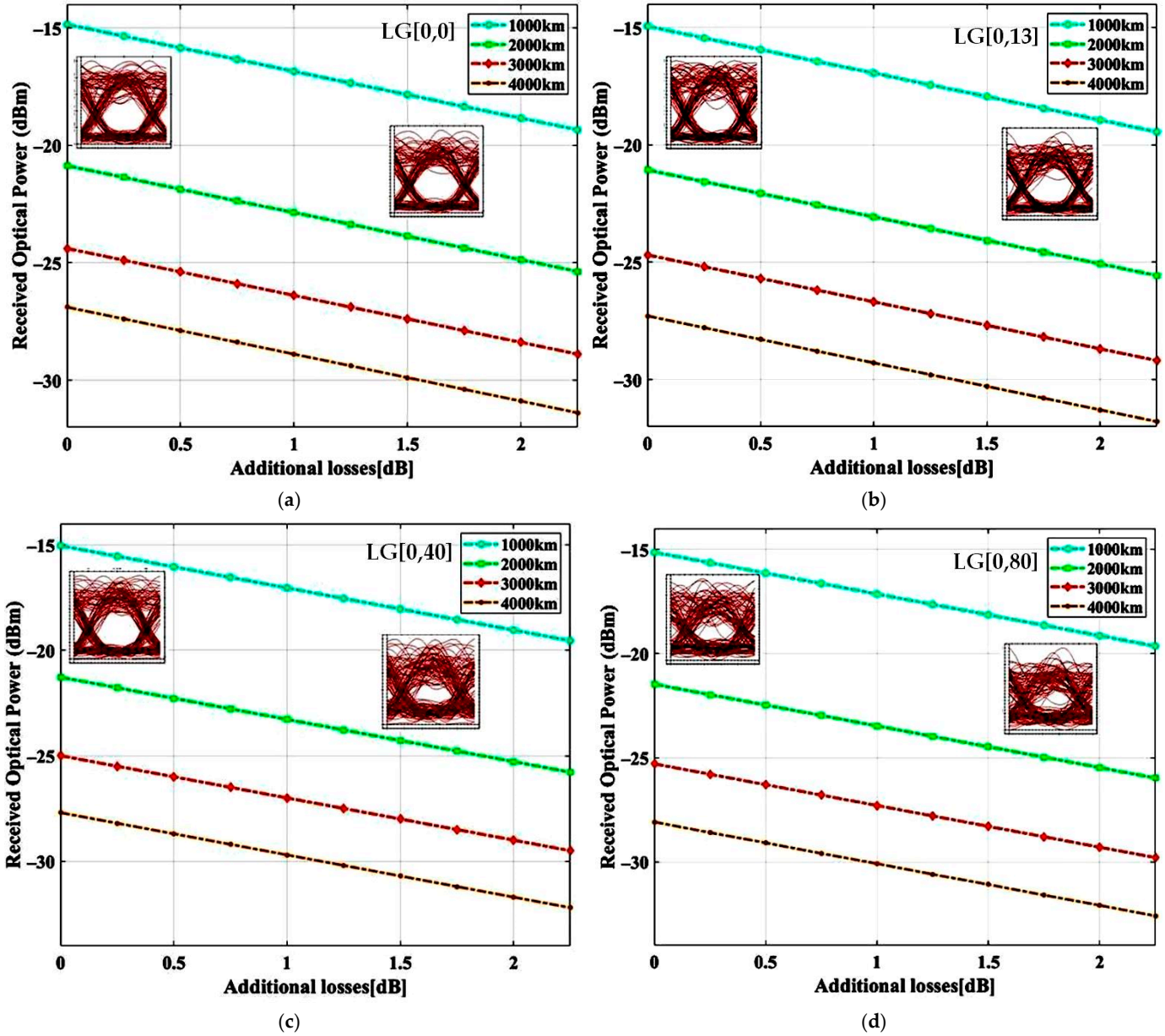

Figure 5. Received power versus additional losses for operating modes of (**a**) LG [0,0], (**b**) LG [0,13], (**c**) LG [0,40] and (**d**) LG [0,80]; corresponding eye patterns at 0.5 and 2 dB losses.

For all modes at 1000 km, Figure 5a–d shows inset eye patterns at 0.5 and 2 dB losses. Increasing the operating mode from a fundamental to a higher one decreases the performance of the system. LG [0,0] mode produces clear and wide eye patterns. Additionally, eye patterns are better at the 0.5 dB additional loss than at the 2 dB loss. Table 3 shows the received power over different modes and wavelengths at the 2.5 dB loss for different modes and wavelengths.

Table 3. Received power for different modes over varied range at 2.5 dB additional loss.

	Received Power (dBm)			
Range (km)	**LG [0,0]**	**LG [0,13]**	**LG [0,40]**	**LG [0,80]**
1000	−19.34	−19.45	−19.54	−19.64
2000	−25.37	−25.57	−25.77	−25.97
3000	−28.37	−29.19	−29.49	−29.79
4000	−31.39	−31.79	−32.19	−32.59

Further, based on varied pointing errors at the transmitter at the 1000 km range, Table 4 illustrates the system's performance at LG [0,0] mode in terms of gain, input−output received signal, SNR, and OSNR. As the pointing error increases, the system's performance decreases. Maximum gain, output signal power, SNR and OSNR of −40.80 to −41.12 dB, −14.26 to −14.58 dBm, 55.21 to 54.59 dB and 67.25 to 66.63 dB are obtained, respectively, at LG [0,0] mode for the 0.1–0.9μrad pointing error at the transmitter.

Table 4. Obtained results for LG [0,0] mode.

Tx Pointing Error (μrad)	**Gain (dB)**	**Input Signal (dBm)**	**Output Signal (dBm)**	**SNR (dB)**	**OSNR (dB)**
0.1	−40.80	26.53	−14.26	55.21	67.25
0.3	−40.83	26.54	−14.28	54.83	66.87
0.5	−40.89	26.54	−14.35	54.60	66.64
0.7	−40.99	26.54	−14.45	54.79	66.83
0.9	−41.12	26.54	−14.58	54.59	66.63

Figure 6a–f illustrates the obtained spectra of the system for different components. Figure 6a depicts the obtained optical spectrum at the transmitter side and represents four different wavelengths from 1550–1552.4 nm at the input power of 10 dBm. After mode signals transmission over an OWC link range of 5000 km, optical power is reduced to −20 dBm, as depicted in Figure 6b. This happens due to the impact of OWC link impairments like a geometric loss, a pointing loss of 0.1 μrad and an additional loss of 0.5 dB. Figure 6c illustrates the clear and symmetric time sequence output spectrum in the oscilloscope visualizer at the transmitter side, while a distorted time sequence output spectrum is obtained at the receiver after a 5000 km transmission, as presented in Figure 6d. Furthermore, the impact of using a Bessel filter is also illustrated in Figure 6e,f. It is clear that by utilizing the Bessel filter, high-quality signals are obtained and thus the signal quality is improved.

A system's EVM can specifically determine the degree of damage to the received signals. It is defined as the vector mean square ratio between reference and measured signals [20,21]. For different operating modes and wavelength signals, Figure 7a–d shows the EVM% in terms of different ranges. Under the EVM threshold of 17.5%, the LG [0,0] mode shows the best performance with less EVM and a greater transmission range. Figure 7a shows the EVM% for LG [0,0] mode at 1550 nm, 3.34–18.46% at 1550.8 nm, 3.04–18.50% at 1551.6 nm, and 3.57–18.31% at 1552.4 nm. According to Figure 7b, LG [0,13] achieves an EVM% of 3.01–18.36% at 1550 nm, 3.74–18.22% at 1550.8 nm, 3.23–18.24% at 1551.6 nm, and 3.61–18.37% at 1552.4 nm over 500–3500 km. Furthermore, LG [0,40] and LG [0,80] exhibit an EVM% of 3.65–18.33% and 3.08–18.38% at 1550 nm, 3.59–18.26% and 3.71–18.47% at 1550.8 nm, 3.16–18.38% and 3.11–18.45% at 1551.6 nm, and 3.08–18.89% and 3.57–18.43% at 1552.4 nm, respectively. OAM modes after the 1000 km range are also shown in Figure 7a–d.

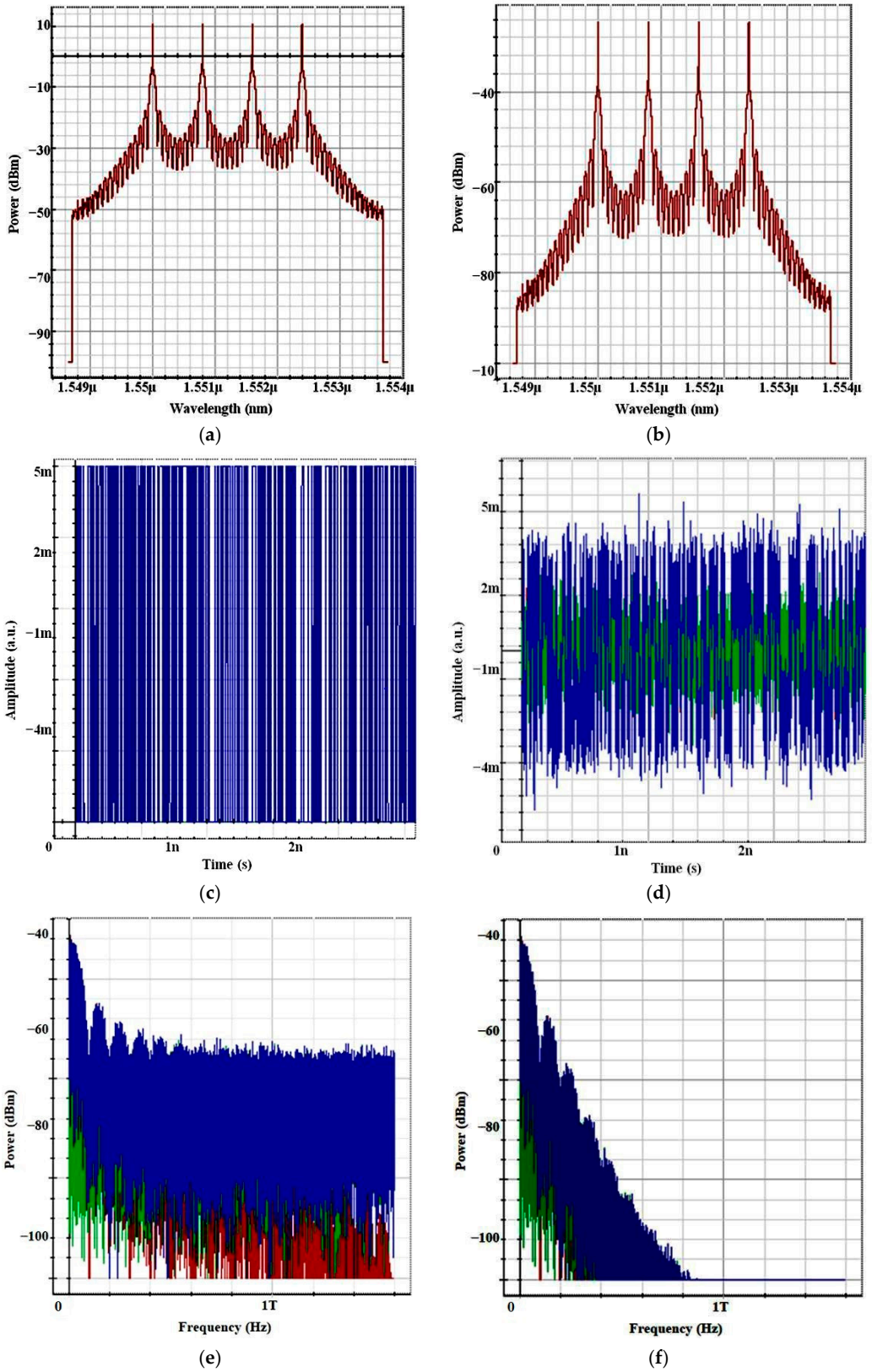

Figure 6. Obtained outputs (**a**) optical spectrum at Tx, (**b**) optical spectrum at Rx, (**c**) oscilloscope visualizer spectrum at Tx, (**d**) oscilloscope visualizer spectrum at Rx, (**e**) RF spectrum before Bessel filter and (**f**) RF spectrum after Bessel filter.

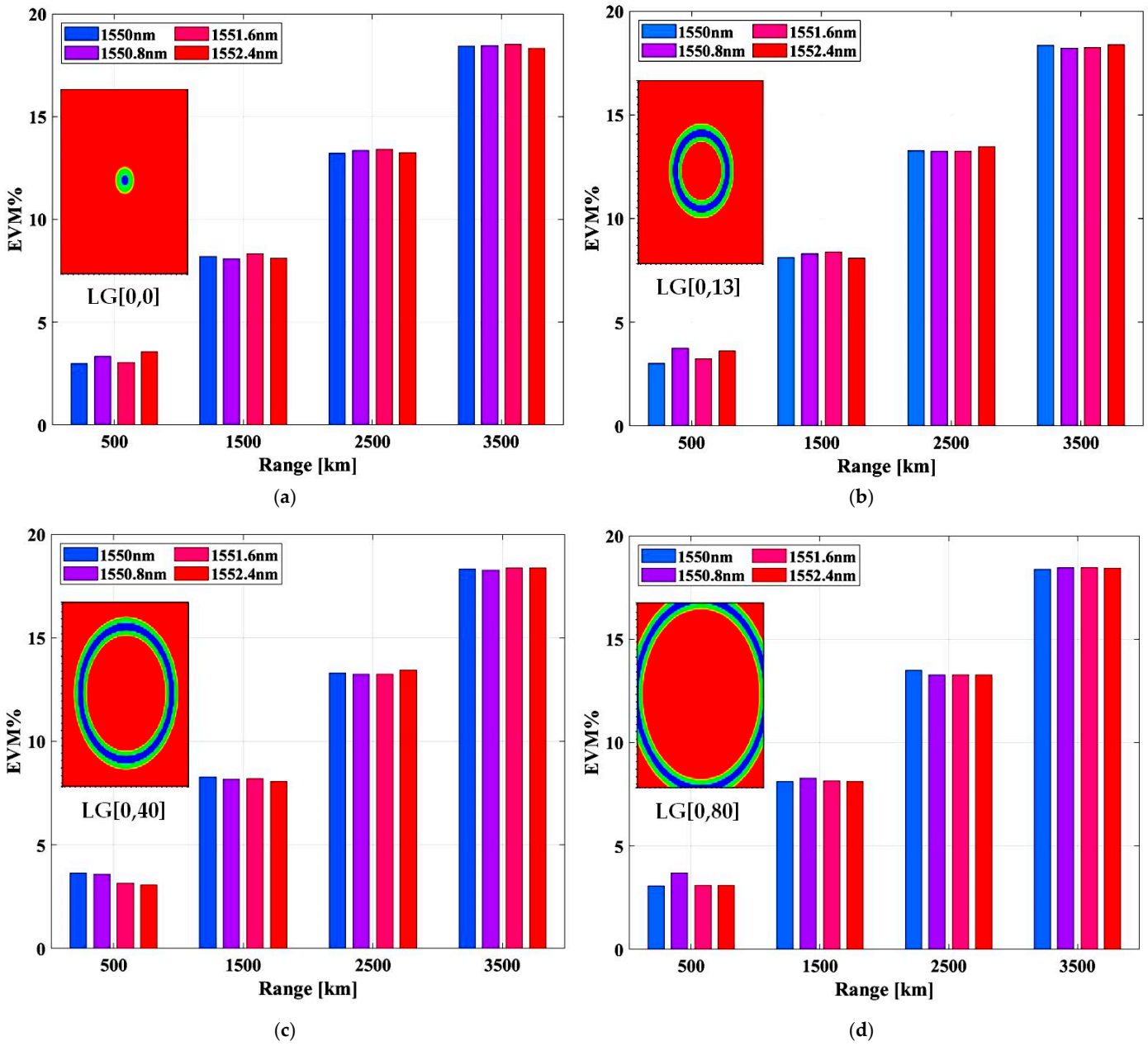

Figure 7. EVM% versus range for operating modes of (**a**) LG [0,0], (**b**) LG [0,13], (**c**) LG [0,40] and (**d**) LG [0,80] for different wavelengths; Insets: corresponding OAM modes.

Table 5 depicts the performance analysis of the system in terms of the EVM% for various modes at the 1000–5000 km range. At a threshold value of 17.5% EVM for the 4-QAM modulation format, an approximately 4500 km range can obtained for all modes. However, the best performance can be obtained for LG [0,0] mode, which is followed by LG [0,13], LG [0,40], and LG [0,80].

Table 5. EVM% for varied transmission range at diverse operating modes.

Range (km)	LG [0,0]	LG [0,13]	LG [0,40]	LG [0,80]
1000	5.53	5.51	5.52	5.60
2000	10.68	10.76	10.77	10.89
3000	15.80	15.84	15.84	15.80
4000	20.86	20.80	20.78	20.81
5000	25.94	25.86	25.68	25.75

In Table 6, the proposed work is compared with existing ones, and it is realized that the proposed work offers the highest wireless range of 5000 km at an aggregate 800 Gbps throughput at a high SNR of 55 dB.

Table 6. Comparison performance w.r.t. existing works.

Refs.	No. of Modes	Mode	Data Rate (Gbps)	Wireless Range (km)	Turbulent Condition	No. of Channels	SNR (dB)	BER	Complexity and Cost	Applications
[20]	Not used	Not used	0.0126	500	Weak, moderate, strong	2	Not defined	10^{-3}	Moderate	Internet of things
[21]	4	01, 02, 03, 04	2.488	Not used	Not used	4	Not defined	10^{-9}	High	Short distance-local area network
[22]	2	00, 01	20	1750	Not defined	6	Not defined	10^{-9}	High	Secure wireless network
[23]	Not used	Not used	0.622	500	Moderate	3	22	10^{-9}	Moderate	Tri-play services
[24]	9	00, 01, 02, 10, 11, 12, 20, 22, 21	10	3200	Not defined	10	Not defined	10^{-9}	Moderate	Fiber to the home
[25]	3	01, 02, 03	1.866	Not used	Not used	3	Not defined	10^{-9}	High	Hybrid wired-wireless networks
[26]	Not used	Not used	Not defined	1.5 k	Weak-strong	Not defined	36	10^{-3}	Moderate	Secure wireless network
[27]	Not used	Not used	10	160	Not used	Not defined	Not defined	10^{-9}	High	Hybrid wired-wireless networks
This work	4	0,0; 0,13; 0,40; 0,80	200	5000	Moderate	4	55	10^{-3}	Medium	High speed and high capacity satellite-to-ground communication

5. Conclusions

A 4 × 200 Gbps OFDM-OWC system using OAM multiplexing is presented for HAP-to-satellite communication. There are four higher-order OAM modes, namely LG mode at [0,0], [0,13], [0,40], and [0,80], to enhance the system performance over long-range and high-throughput OWC links. System performance is evaluated for four operating wavelengths of 1550, 1550.8, 1551.6, and 1553.2 nm. Under transmission pointing errors, geometric loss, turbulence, and additional link losses, the system offers a faithful 5000 km at LG [0,0] and LG [0,13] modes. While for LG [0,40] and LG [0,80] modes, a maximum 4700–5000 km and 3300–4000 km transmission range is obtained at aggregate data traffic of 800 Gbps. According to constellation diagrams, eye patterns, and optical spectra, LG [0,0] has the best performance. Additionally, it is possible to obtain −19.34 to −31.39 dBm for LG [0,0], −19.45 to −31.79 dBm for LG [0,13], −19.54 to −32.19 dBm for LG [0,40] and −19.64 to −32.59 dBm for LG [0,80] modes over a 1000–4000 km range in the system having an

additional loss of 2.5 dB. Moreover, the EVM% ranges from 5.53 to 25.94 for LG [0,0], 5.51 to 25.86 for LG [0,13], 5.52 to 25.68 for LG [0,40], and 5.60 to 25.75 for LG [0,80] OAM modes. In addition, 4 QAM threshold EVM% of 17.5% can be observed over a 3500 km range for all modes. For varied pointing errors, the system offers a high gain, SNR, output signal, and OSNR of −40.80 dB, 55.21 dB, −14.26 dBm, and 67.25 dB, respectively. Under moderate turbulence, this system offers better performance in terms of high channel capacity (=4), data rate (=200 Gbps), and range (=5000 km) with moderate complexity as well as cost. The system can be used in the future for long-range satellite-to-ground transmissions and vice versa.

Author Contributions: M.K. and S.K.M. discussed the plan and agreed on it. M.K. drafted designs for the manuscript. The manuscript original was written by M.K. The manuscript was edited by S.K.M. All authors reviewed and commented on the original draft of the manuscript. All authors have read and agreed to the published version of the manuscript.

Funding: S.K.M. wants to thank CTTC for providing the resources to conduct this research.

Institutional Review Board Statement: Not applicable.

Informed Consent Statement: Not applicable.

Data Availability Statement: Data are contained within the article.

Conflicts of Interest: The authors declare no conflicts of interest.

References

1. Kong, H.; Lin, M.; Zhu, W.P.; Amindavar, H.; Alouini, M.S. Multiuser Scheduling for Asymmetric FSO/RF Links in Satellite-UAV-Terrestrial Networks. *IEEE Wirel. Commun. Lett.* **2020**, *9*, 1235–1239. [CrossRef]
2. Nguyen, T.V.; Le, H.D.; Dang, N.T.; Pham, A.T. On the Design of Rate Adaptation for Relay-Assisted Satellite Hybrid FSO/RF Systems. *IEEE Photonics J.* **2022**, *14*, 1–11. [CrossRef]
3. Liu, X.; Lin, M.; Zhu, W.P.; Wang, J.Y.; Upadhyay, P.K. Outage Performance for Mixed FSO-RF Transmission in Satellite-Aerial-Terrestrial Networks. *IEEE Photonics Technol. Lett.* **2020**, *32*, 1349–1352. [CrossRef]
4. Refaai, A.; Fathi, M.; Sree, A.; Newagy, F.; Aly, M.H.; Elhennawy, H. Cooperative Relay Orbital Satellite Optical Communication under Turbulent Channels: Performance Analysis. *Opt. Laser Technol.* **2023**, *161*, 109110. [CrossRef]
5. Ju, C.; Liu, N.; Zhang, Z.; Chen, X. A Flexible Optical OFDMA-PON Upstream Scheme Based on Modulation Format Conversion Technique. *Opt. Laser Technol.* **2017**, *90*, 237–241. [CrossRef]
6. Dong, Y.; Giddings, R.P.; Tang, J. Hybrid OFDM-Digital Filter Multiple Access PONs. *J. Light. Technol.* **2018**, *36*, 5640–5649. [CrossRef]
7. Lee, D.; Sasaki, H.; Fukumoto, H.; Hiraga, K. Orbital Angular Momentum (OAM) Multiplexing: An Enabler of a New Era of Wireless Communications. *IEICE Trans. Commun.* **2017**, *100*, 1044–1063. [CrossRef]
8. Dutta, B.; Sarkar, N.; Atta, R.; Kuiri, B.; Sekhar, A. 1600 Gbps PAM-4 FSO Link Enabled Using OFCL-Based WDM and OAM-Multiplexing Techniques. *Results Opt.* **2022**, *9*, 100287. [CrossRef]
9. Liu, J.; Lin, Z.; Zhu, H.; Shen, L.; Mo, S.; Li, Z.; Zhang, J.; Zhang, J.; Lan, X.; Liu, J.; et al. 1120-Channel OAM-MDM-WDM Transmission over a 100-Km Single-Span Ring-Core Fiber Using Low-Complexity 4 × 4 MIMO Equalization. *Opt. Express* **2022**, *30*, 18199. [CrossRef]
10. Li, S.; Wang, J. Adaptive Power-Controllable Orbital Angular Momentum (OAM) Multicasting. *Sci. Rep.* **2015**, *5*, 9677. [CrossRef]
11. Rjeb, A.; Fathallah, H.; Khaled, I.; Machhout, M.; Alshebeili, S.A. A Novel Hyperbolic Tangent Profile for Optical Fiber for Next Generation OAM-MDM Systems. *IEEE Access* **2020**, *8*, 226737–226753. [CrossRef]
12. Arum, S.C.; Grace, D.; Mitchell, P.D. Delivering Extended Cellular Coverage and Capacity Using High-Altitude Platforms. *Electronics* **2022**, *11*, 1508. [CrossRef]
13. Erdogan, E.; Yahia, O.B.; Kurt, G.K.; Yanikomeroglu, H. Optical HAPS Eavesdropping in Vertical Heterogeneous Networks. *IEEE Open J. Veh. Technol.* **2023**, *4*, 208–216. [CrossRef]
14. Wang, X.; Zhao, S.; Shi, L.; Li, Y.; Zhao, G.; Zhu, Z.; Zhao, W. Error Rate Performance Analysis of Optical Links between High Altitude Platforms with Misalignment Fading by Hoyt Distribution. *Optik* **2013**, *124*, 6516–6518. [CrossRef]
15. Swaminathan, R.; Sharma, S.; Vishwakarma, N.; Madhukumar, A.S. HAPS-Based Relaying for Integrated Space–Air–Ground Networks with Hybrid FSO/RF Communication: A Performance Analysis. *IEEE Trans. Aerosp. Electron. Syst.* **2021**, *57*, 1581–1599.
16. Sachdeva, S.; Kaur, S.; Arora, R.; Sindhwani, M.; Arora, K.; Cho, W.; Joshi, G.P.; Doo, I.C. Ultra-High Capacity Optical Satellite Communication System Using PDM-256-QAM and Optical Angular Momentum Beams. *Sensors* **2023**, *23*, 786. [CrossRef] [PubMed]
17. Kumari, M.; Arya, V. Realization of High-Speed OWC Links by Incorporating Hybrid OCDMA and MDM Scheme for HAP-to-Satellite Applications. *Opt. Quantum Electron.* **2024**, *56*, 546. [CrossRef]

18. Fontaine, N.K.; Ryf, R.; Chen, H.; Neilson, D.T.; Kim, K.; Carpenter, J. Laguerre-Gaussian Mode Sorter. *Nat. Commun.* **2019**, *26*, 1865. [CrossRef]
19. Banawan, M.; Mishra, S.K.; Gouin, A.; Bacon, N.; Guan, X.; Wang, L. Using Standard 2 × 2 MIMO to Increase Capacity of Spatial Multiplexing with OAM Modes. *J. Light. Technol.* **2023**, *41*, 1974–1984. [CrossRef]
20. Pesek, P.; Zvanovec, S.; Chvojka, P.; Ghassemlooy, Z.; Haigh, P.A. Demonstration of a Hybrid FSO/VLC Link for the Last Mile and Last Meter Networks. *IEEE Photonics J.* **2019**, *11*, 1–7. [CrossRef]
21. Ghazi, A.; Aljunid, S.A.; Idrus, S.Z.S.; Fareed, A.; Al-Dawoodi, A.; Mohsin, A.H. Design of a Hybrid WDMA-Optical-CDMA over Multi-Mode Fiber Transmission System Based on LG Modes for Short Haul-Local Area Network. *J. Phys. Conf. Ser.* **2021**, *1793*. [CrossRef]
22. Sarangal, H.; Nisar, K.S.; Thapar, S.S.; Singh, A.; Malhotra, J. Performance Evaluation of 120 GB/s Hybrid FSO-SACOCDMA-MDM System Using Newly Designed ITM-Zero Cross-Correlation Code. *Opt. Quantum Electron.* **2021**, *53*, 64. [CrossRef]
23. Mostafa, S.; Mohamed, A.E.A. Performance Evaluation of SAC-OCDMA System in Free Space Optics and Optical Fiber System Based on Different Types of Codes. *Wirel. Pers. Commun.* **2017**, *96*, 2843–2861. [CrossRef]
24. Ghazi, A.; Aljunid, S.A.; Noori, A.; Idrus, S.Z.S.; Rashidi, C.B.M.; Al-Dawoodi, A. Design & Investigation of 10 × 10 Gbit/s MDM over Hybrid FSO Link under Different Weather Conditions and Fiber to the Home. *Bull. Electr. Eng. Inform.* **2019**, *8*, 121–126. [CrossRef]
25. Ghazi, A.; Aljunid, S.A.; Syed Idrus, S.Z.; Fareed, A.; Rashidi, C.B.M.; Al-Dawoodi, A. Comparison of Laguerre-Gaussian and Hermite-Gaussian Modes for Optical-CDMA over Multi-Mode Fiber. *IOP Conf. Ser. Mater. Sci. Eng.* **2020**, *767*. [CrossRef]
26. Srivastava, V.; Mandloi, A.; Soni, G.G. Outage Probability and Average BER Estimation of FSO System Employing Wavelength Diversity. *Opt. Quantum Electron.* **2019**, *51*, 229. [CrossRef]
27. Yeh, C.H.; Lin, W.P.; Luo, C.M.; Xie, Y.R.; Chang, Y.J.; Chow, C.W. Utilizing Single Lightwave for Delivering Baseband/Fso/Mmw Traffics Simultaneously in Pon Architecture. *IEEE Access* **2019**, *7*, 138927–138931. [CrossRef]